5 Hexagonal and non-hexagonal carbon surfaces

I. László
Department of Theoretical Physics, Institute of Physics, Budapest University of
Technology and Economics, H-1521 Budapest, Hungary

Abstract

We review the most important experimental and theoretical results obtained for fullerenes, nanotubes, various hexagonal and non hexagonal 2 dimensional carbon materials, Haeckelite structures and nanotube junctions. We present various algorithms for generating the connectivity structures and the Descartes coordinates of the carbon atoms. We present that the topological coordinate method can give good Descartes coordinates for fullerenes nanotubes, toroidal, helical and planar arrangement of carbon atoms. Two algorithms is presented for constructing junctions between nanotubes of any chirality and diameter.

Correspondence/Reprint request: Dr. I. László, Department of Theoretical Physics, Institute of Physics Budapest University of Technology and Economics, H-1521 Budapest, Hungary

1. Introduction

In the study of various carbon structures is inevitable the calculation of the Cartesian coordinates of the   atoms. We need them in the study of mechanical and electronic properties as well. One can find difficulties even in the case of fullerenes. These difficulties are grater in the case of more complicated surfaces with positive and negative Gaussian curvatures. Usually only the topological arrangement of the atoms is given by the neighboring structure of the atoms, but we need the Cartesian coordinates as well. A widely used procedure is to set a molecular mechanics program to minimize some parametrized potential energy function using the bonding connectivity as an input parameter. A much simpler approach is the topological coordinate method. An other task is the generation of the connectivity structure at nanotube junctions. There are several theoretical propositions for this problem, but most of them are applied for non chiral tubes that is for nanotubes with a mirror plane.

On carbon surface we mean such kind of atomic arrangement of carbon atoms where the atoms are on a 2 dimensional (2-D) surface.

In mathematics 2 dimensional manifolds are used for describing two dimensional curved surfaces. The Gaussian curvature, or simply the curvature, of a surface is a measure of its intrinsic geometry. The curvature at a point is defined as the inverse of the radius of the best fitting circle to a given curve at this point. On a 2-D surface the maximum and minimum values of this curvature at a point are called principal curvatures k_1, k_2 in order. The Gaussian curvature $k = k_1 \cdot k_2$ is the product of the two principal curvatures. The plane and the cylinder both of them have Gaussian curvatures $k = 0$ and they can be covered by hexagonal carbon structures resulting the graphene sheets and the carbon nanotubes. The Gaussian curvature of the sphere is positive   ($k > 0$), and for constructing the spherical fullerenes we need 12 pentagons as well. Positive Gaussian curvature can not be obtained using only hexagonal structures. If the number of the atoms in a polygon is greater than six we can obtain the surfaces with negative Gaussian curvature. Such kind of surfaces have saddle points. At saddle points the center of the two best fitting circles are at different sides of the surface.

In the next paragraphs after reviewing the experimental and theoretical results on the topics of carbon surfaces, first we describe some geometrical and topological properties of these structures. That is carbon structures where the carbon atoms are on curved surfaces. Then the topological coordianate method will be presented for fullerenes, toroidal, helical and hexagonal nanotubes and planar carbon surfaces. In these paragraphs it will be shown that applying only the neighboring structure of the atoms, their Cartesian coordinates can be generated and we can have some insight even into the electronic structure of

the carbon material under study. In the next paragraph an algorithm will be presented for constructing Y and T –like junctions between two single wall nanotubes of any chirality and diameter. This algorithm is based on the geometric intersection of cylinders and it can describe most of the Y junctions obtained by the Ti-doped vapor catalyst method [62]. The following paragraph will contain an other algorithm for constructing junctions between nanotubes of any chirality. This method is based on the terminology of manifolds and on the local coordinates. In this method the neighboring structure of the atoms at the junction will be obtained as solutions of diophantic equations.

2. Experimental and theoretical results for carbon surfaces

2.1 Fullerenes

During experiments aimed at understanding the mechanisms by which long-chain carbon molecules are formed in interstellar space and circumstellar shells, graphite has been vaporized by laser irradiation, producing a remarkably stable cluster consisting of 60 carbon atoms [1]. It turned out that by this experiment Kroto et al. have found a new allotrope form of carbon. This molecule has the form of the European football or of a truncated icosahedron, that is a polygon with 60 vertices and 32 faces, 12 of which are pentagonal and 20 hexagonal. Each carbon atom has three neighbors just like in the graphite, but the structure has a cage like form of curved surface. After the architect Buckminster-Fuller the inventors gave the name Buckminster-fullerene to this C_{60} molecule. In the following years several other cage like carbon molecules were found. Each of them contain 12 pentagons and several hexagons. Now they are called fullerenes [2]. Putting pentagons into the hexagonal graphitic networks of carbon atoms the planar graphene sheet turned to be a curved surface. Here we imagine the bulk graphite as parallel graphene sheets. Krätschmer et al. [3] has synthesized the bulk form of the C_{60} molecule opening the way to new possibilities of fullerene researches.

2.2 Nanotubes

Iijima [4] has found that curved surfaces can be formed also by imagining rolling up graphene sheets to cylinders, thus forming nanotubes of different chiralities. In the ideal case nanotubes have only hexagonal surface polygons. These needle-like tubes were produced in arc-discharge evaporation method similar to that used for fullerene synthesis [3]. Carbon-arc synthesis produces almost entirely multi wall nanotubes (MWNT). The multi wall nanotubes are formed on the carbon cathode and the single wall nanotubes (SWNT) grow in the gas phase [5,6]. Arc-discharge [7,8], laser ablation [9] and chemical vapor

depositions (CVD) [10] are the main methods for single wall nanotube production and they usually grow with catalytic particles. The HiPCO produces SWNTs by high-pressure catalytic decomposition of carbon monoxide [11].

2.3 Periodic version of fullerenes

Mackay and Terrones [13-15] proposed that assuming rings of 5, 7, and 8 carbon atoms, in graphitic sheets, a great variety of finite and infinite structures can be postulated. Besides the shells of fullerenes, which have positive Gaussian curvature and the cylinders which have zero Gaussian curvature, infinite periodic networks with negative Gaussian curvatures are possible. They have discussed the geometric and physical properties of these hypothetical periodic graphite foams and they have found them more stable than the C_{60} molecule. Vanderbilt and Tersoff [16] have constructed a periodic analog of C_{60}, the C_{168} periodic carbon network. The unit cell of this structure contains 168 carbon atoms and every atom is in a topologically equivalent local environment participating in one seven fold and two six fold rings. Namely the periodic C_{168} structure is obtained from the C_{60} by replacing the pentagons by heptagons and thus changing the positive Gaussian curvature to a negative one. They have calculated that the C_{168} has less formation energy than the C_{60} as its bond angles are closer to 120° than the angles of the C_{60} fullerene. The stability of similar periodic structures was studied by Lenosky et al. [17].

2.4 Toroidal and helical structures

Dunlap [18] has shown that different hexagonal carbon nanotubes can be connected together in a several number of ways using heptagon pentagon pairs. The stability of these joints was indicated by the fact that the binding energies of finite tori made using twelve such joints are bracketed by the binding energies of the two corresponding infinite tubes. Itoh, Ihara and Kitakami suggested a series of toroidal structures C_{120}, C_{360}, C_{480}, C_{840}, C_{1080}, C_{1440}, C_{1560} and C_{1920} containing fivefold six-fold and sevenfold carbon rings [19-20]. These structures have local topological structures of positive and negative Gaussian curvatures corresponding to the positions of pentagons and heptagons respectively. The same authors suggested helically coiled forms of nanotubes by appropriate distribution of pentagons heptagons and hexagons [21]. Toroidal and helical structures containing only pentagons and heptagons has been describet by László and Rassat [22-24].

While examining laser-grown single-wall carbon nanotube materials by scanning force and transmission electron microscopy Liu et al. observed circular formations of single wall nanotube ropes. They were convinced that many of the individual tubes in the circular ropes were perfect tori [25].

Ahlskog et al. observed ring formations from catalytically synthesized carbon nanotubes [26]. Martel, Shea and Avouris have found that single walled carbon nanotubes can be induced to organize themselves into rings or coils [27]. It was shown by Sano et al. that applying covalent ring closure reactions to commercially available carbon nanotubes ring shaped tubes can be obtained [28]. Further ring structures can be found in references [29,30].

Amelinckx et al. studied the formation mechanism for catalytically grown helix shaped graphite nanotubes [31].

2.5 Haeckelite structures and nanocones

Terrones et al [32] incorporating five-, six-, and seven-membered rings in two dimensional carbon lattices proposed a new family of layered sp^2-like carbon crystals., named Haeckelites. According their definition these crystals consist of equal numbers of pentagons and heptagons, in addition to any number of hexagons. The authors have studied three specific examples with different symmetries. All of them were found more stable than the C_{60} molecule. Because of the intrinsic metallic behavior of the Haeckelite sheets under study, all the tubes with any chirality and diameter were found metallic. Classical hexagonal nanotubes can be metallic or semiconductor depending on the chyrality.

Using pentagons and heptagons in a hexagonal lattice also nanocones has been suggested as possible carbon surfaces [33,34]. Graphitic cones has been produced by carbon condensation on graphite substrate [35], by pyrolysis of heavy oils [36] and by laser ablation of graphite targets [37].

2.6 Nanotube junctions and peapods

Scuseria [38] and Chernozatonskii [39] have shown that with the help of extra heptagons nanotube junctions can be constructed. Single walled nanotube junctions between nanotubes of any chirality and diameter has been shown by László [40-43]. Zhou and Seraphin observed L, Y and T patterns of nanotube branching produced from carbon arc-discharge by a graphitic anode with a hollow core in the center [44]. Nagy et al. observed Y-branching by scanning tunneling microscopy in single wall carbon nanotubes grown by thermal decomposition of C_{60} molecules [45,46]. Various nanotube branches were produced by pyrolysis as well [47-49]. Scanning tunneling microscopy (STM) and scanning tunneling spectroscopy (STS) measurements were published on a Y-branched carbon nanotube in ref. [50,51].

Replacing the carbon-carbon bonds of a carbon architecture by SWNTs and the carbon atoms by Y junctions super carbon architectures can be generated. Such kind of carbon nanotube networks were suggested by Coluci et al. [52,53].

An other interesting carbon structures were found in 1998 the peapods [54]. We call peapods the encapsulated C_{60} molecules in carbon nanotubes.

Also the abovementioned examples show that carbon assumes a wide variety of different structures and forms. Each of them have unique physical and chemical properties giving potential applications in several fields [55]. Single wall carbon nanotubes have extraordinary mechanical properties. They can be used as reinforcement in composites. Their size and electronic properties make them possible building blocks in nano electronics and applications in display and gas sensor production [56]. There are other special review articles about mechanical and electrical properties of nanotubes [57], structural properties of Haeckelite nanotubes [58], curved nanostructured materials [59], three-terminal junctions of carbon nanotubes [60,61].

3. Geometry of the C_{60} molecule and hexagonal nanotubes
3.1 The C_{60} molecule

We call a carbon structure carbon surface if the carbon atoms can be imagined being on a 2-dimensional surface. Thus the simplest carbon surface is the graphene sheet. The first curved carbon structure was found by production of the C_{60} molecule where the 60 carbon atoms are on the surface of a sphere [1]. This structure can be imagined as a truncated icosahedron (Figure 1.b.). In Figure 1.a. we can see a regular icosahedron. The regular icosahedron is one of the five platonic polyhedron. It has 12 vertices, 30 edges and 20 equilateral triangles. A regular icosahedron with edge distance of 2 is given for example by the coordinates $(0,\pm\tau,\pm1)$, $(\pm1,0,\pm\tau)$ and $(\pm\tau,\pm1,0)$, where $\tau = \left(1+\sqrt{5}\right)/2$ is the golden ratio (Figure 1a). The truncated icosahedron is obtained from the icosahedron by cutting off a pentagonal pyramid at each vertices (Figure 1.b). The Cartesian coordinates of the truncated icosahedron are calculated from those of the icosahedron in the following way. Let $\mathbf{r}_a$ and $\mathbf{r}_b$ be the position vectors of two neighboring vertices of the icosahedron. The corresponding edge generate two vertices of the truncated icosahedron by the relations $\mathbf{r_1} = \mathbf{r_a}(1\text{-}q)+\mathbf{r_b}q$ and $\mathbf{r_2} = \mathbf{r_a}q + \mathbf{r_b}(1\text{-}q)$, where $0 < q < 0.5$ is a real number. As the icosahedron has 30 edges the truncated icosahedron will have 60 vertices. As there are 12 vertices in the icosahedron the truncated icosahedron has 12 pentagons. Its 20 hexagons are obtained from the 20 regular triangles.

In Figure 1.b we can see that there are two kinds of edges on the truncated icosahedron, the edges between two hexagons and the edges between a hexagon and a pentagon. They have the same length for $q = \frac{1}{3}$.

Kroto et al has produced the C_{70} molecule as well [1]. As it was mentioned before there has been found other cage like molecules which are now called, the fullerenes. Each of them have 12 pentagons and several hexagons.
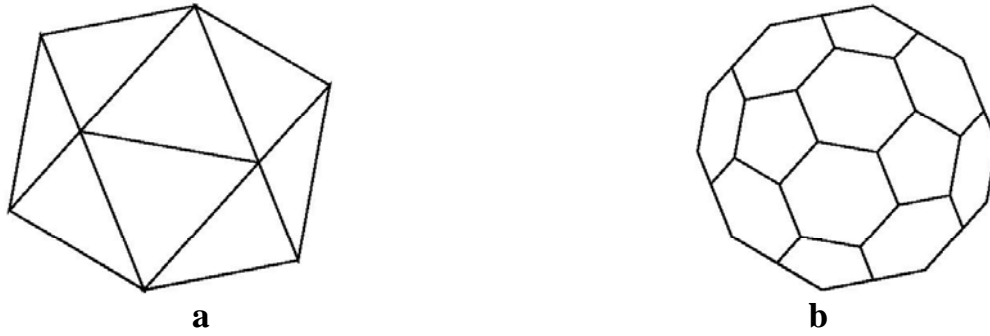
Figure 1.   Regular icosaderon (a) and the truncated icosahedron (b).

3.2 Hexagonal nanotubes

Introducing two unit vectors $\mathbf{a_1} = a(\sqrt{3},0)$ and $\mathbf{a_2} = a\left(\dfrac{\sqrt{3}}{2},\dfrac{3}{2}\right)$ with inter atomic distance a on the graphene sheet and two integers k and 1 we can assign coordinates (k,1) to each hexagon of the sheet (Figure 2.a). This coordinate system gives the position of each hexagon on the honeycomb lattice. Namely the center of the hexagon (k,1) is at the end of the position vector $R = k\,a_1 + a_2$. The unit vectors a_1 and a_2 define also the unit cell of the hexagonal lattice containing two carbon atoms of indices r = 1 and r = 2. Thus the two integers k and 1 are also the coordinates of the translated unit cells as well and (k,1,r) means the r-th atom in this unit cell.

On the hexagonal lattice the corresponding points of two parallel lines translated by an position vector $R = k\,a_1 + 1a_2$ lattice vector see the same environment. By identifying them we can construct a cylinder by rolling up the lattice cut out by these lines.   This is why the hexagonal nanotubes are defined with the help of the chiral vector $\mathbf{C_h}$
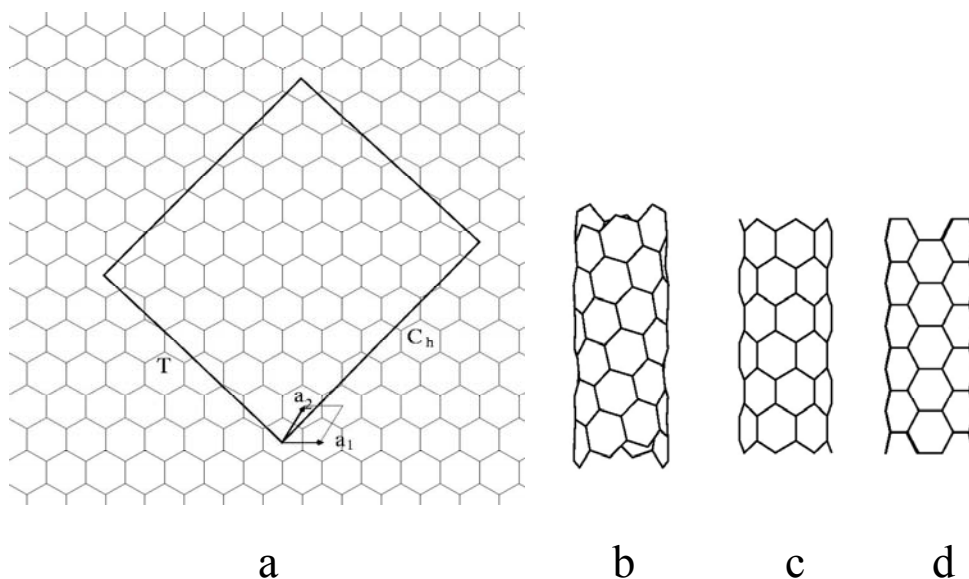
$$\mathbf{C_h} = m\mathbf{a_1} + n\mathbf{a_2} \tag{1}$$

where m and n are integers (Figure 2.). The chiral vector and the multiple of the translation vector $\mathbf{T}$ defines a rectangle which is the super cell in our rolling up construction. By identifying those two parallel lines of these rectangle which are parallel also with $\mathbf{T}$ one can construct a cylinder. The vector $\mathbf{T}$ is perpendicular to the chiral vector $\mathbf{C_h}$ and defined as

$$\mathbf{T} = \left[-(2n+m)\mathbf{a_1},\,(2m+n)\mathbf{a_2}\right]/d_R \tag{2}$$

where d is the highest common divisor of (m, n), and d_R = d if n-m is not a multiple of 3d and d_R = 3d if n-m is a multiple of 3d [55]. Figure 2a shows quadrangle for constructing the nanotube with the parameters (m, n) = (2,6).

There are some special cases, the zigzag and armchair nanotubes with parameters in order (m,0) and (m, m) nanotubes. These nanotubes have at least one mirror plane. The other nanotubes without a mirror plane are the chiral nanotubes. On Figure 2 we show examples of chiral zigzag and armchair nanotubes.

| a | b | c | d |

Figure 2. (a) Coordinate system on a hexagonal lattice defined by the unit vectors a_1 and a_2. The chiral vector $\mathbf{C}_h = m\mathbf{a}_1 + n\mathbf{a}_2$, and the basic translation vector $\mathbf{T}$ is used for defining the quadrangle for constructing the nanotube with the parameters (m, n) = (2,6). (b) The chiral nanotube (m, n) = (2,6). (c) The zigzag nanotube (m, n) = (7,0). (d) The armchair nanotube (m, n) = (4,4).

4. Topology of carbon surfaces

The Euler formula and its consequences [15,41,63] are very useful in the geometrical construction of fullerenes and other curved carbon surfaces. It states that, for any polyhedron homeomorphic to the sphere there is a relation between the number of faces F, number of edges E and the number of vertices V, as:

$$F - E + V = 2. \tag{3}$$

The genus g of an orientable closed surface is defined as the number of handles and it is 0 for the sphere and 1 for the torus. If we define the Euler characteristic as 2(1-g) we obtain the Poincaré formula (or Euler-Poincare formula) for orientable closed surfaces of higher genus as

$$F - E + V = 2(1 - g). \tag{4}$$

If n_i is the number of faces with *i* vertices on their boundary, and each vertex has 3 neighbors, then:

$$E = \frac{1}{2}\sum_i in_i \ , \quad V = \frac{2E}{3} = \frac{1}{3}\sum_i in_i \ , \quad F = \sum_i n_i \tag{5}$$

and thus the Poincaré formula has the following form

$$\sum_i (6-i)n_i = 12(1-g). \tag{6}$$

There is not any constrain for the number of hexagons. For fullerenes g = 0 and from Equ. (6) we obtain:

$$3n_3 + 2n_4 + n_5 - n_7 - 2n_8 - 3n_9 - 4n_{10} - 5n_{11} - 6n_{12} - 7n_{13} - \ldots = 12. \tag{7}$$

As the right hand side of this Equation equals to the positive number 12 and minimizing the bonding energy we do not allow triangles and squares, the fullerene must have at least 12 pentagons as the coefficient of the other polygons are negative. A nanotube which is closed by two half spheres is also homeomorphic to the sphere and Equ. (7) is valid for nanotubes with two closed ends. In the least strained case one can suppose that it has only 12 pentagons and the other polygons are hexagons, that is each half spheres have six pentagons. A junction of three nanotubes with three closed ends can also be imagined as a surface homeomorphic to the sphere. Because of the previous reasoning the three half spheres have 18 pentagons from Equ. (7) follows that $n_5 - n_7 = 12$ and $n_7 = 6$ if we allow only pentagons and heptagons in the least strained case. Thus a nanotube junction between three polyhex nanotubes must have at least 6 heptagons if only hexagons and heptagons are allowed. It is supposed that the pentagons at the ends are cut off with the three half spheres and we are speaking about a junction between three hexagonal nanotubes of open ends [40,41]. The same results were found in references [63-65]. Using the same ideas we obtain the following general relation for a connected nanotube network with e open ends

$$\sum_i (6-i)n_i = 12(1-g) - 6e. \tag{8}$$

For the special case of nanotube junction of three polyhex and open ended nanotubes g = 0, e = 3 and Equation (8) turns to the relation

$$3n_3 + 2n_4 + n_5 - n_7 - 2n_8 - 3n_9 - 4n_{10} - 5n_{11} - 6n_{12} - 7n_{13} - \ldots = -6 \tag{9}$$

5. Adjacency matrices for describing the connectivity structures

5.1 Fullerenes

We describe the atomic arrangement of a 2-dimensional carbon surface by the graph G = (V, E) where V is the set of vertices i and E is that of the edges

(i, j). The vertices correspond to the carbon atoms and the edges to the first neighbor bonds. The **A** adjacency matrix and its A_{ij} matrix elements are defined by the relations, $A_{ij} = 1$ if $(i, j) \subset E$ and $A_{ij} = 0$ otherwise. From Equations (3) and (5) follows:

$$E = \frac{3}{2}V, \quad F = 2 + \frac{V}{2}.$$ (10)

Thus for fullerenes

$$n_5 = 12, \quad n_6 = F - 12 = \frac{V}{2} - 10.$$ (11)

From practical point of view the simplest way to construct a fullerene polyhedron is based on the following spiral conjecture [2].

Spiral conjecture[2]:*The surface of a fullerene polyhedron may be unwound in a continuous spiral strip of edge-sharing pentagons and hexagons such that each new face in the spiral after the second shares an edge with both (a) its immediate predecessor in the spiral and (b) the first face in the preceding spiral that still has an open edge.*

If the number of vertices V is given, from Equations (10,11) follows the number of faces F, that is the number of pentagons and the number of hexagons. According to the spiral conjecture the spiral of the polyhedron is represented by a one-dimensional sequence of 5s and 6s which give the positions of pentagons and heptagons. The number of 5s is $n_5 = 12$ and the number of 6s is $n_6 = \frac{V}{2} - 10$. The spiral can be given by a series of 12 numbers, where each number is the serial number of a pentagon in the spiral of polygons. Once a tentative spiral sequence of 5s and 6s has been constructed, the next task is to check whether it winds up to give a fullerene or not. If not, one has to try by an other sequence of pentagons and hexagons using the same number of faces F, which is determined by the number of vertices V. In the winding up procedure it is useful to construct the dual of the fullerene under study. The vertices of a polyhedron correspond to the faces of its dual, and vice versa. If the winding up procedure is successful the graph $G = (V, E)$ of the fullerene is constructed and its adjacency matrix **A** can be given. Let us supposed that we want to construct a fullerene C_{100} with V = 100 carbon atoms. From Equ. (10) follows that F = 52.

In Figure 3.a we can see the spiral (1,7,12,19,25,28,30,33,36,41,48,50) of a C_{100} fullerene.

In ref. [2] there are more details about the spiral algorithm and its consequences. This book contains also Fortran computer programs for this method. The spiral conjecture did not failed for constructing fullerenes up to 100

a   b
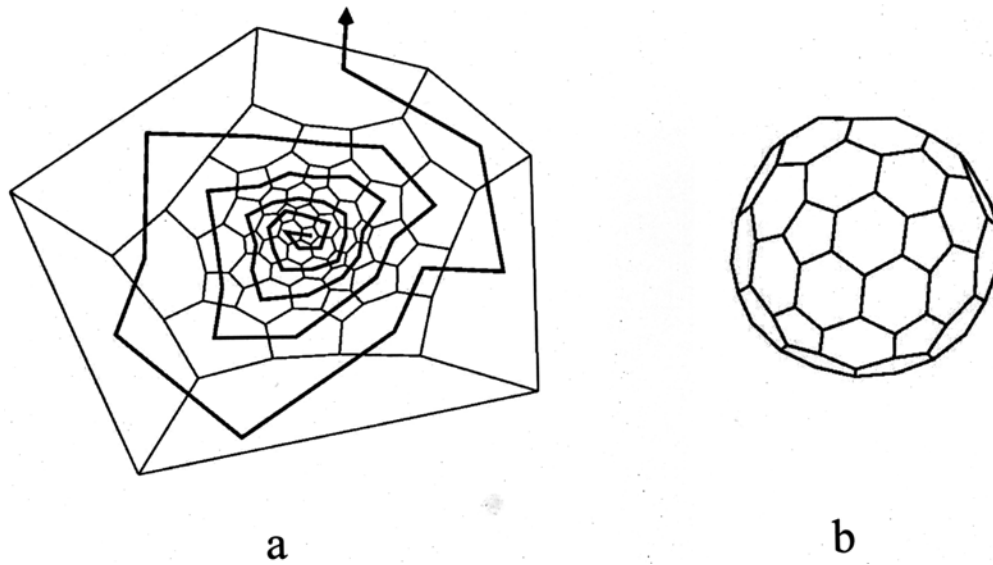
Figure 3. (a) The spiral (1,7,12,19,25,28,30,33,36,41,48,50) of a C_{100} fullerene on its graph G (V, E) obtained by the spiral algorithm and the (b) corresponding C_{100} fullerene.

carbon atoms and the smallest tetrahedral fullerene without a spiral is a C_{380} fullerene [2].

5.2 The adjacency matrix of nanotubes, toroidal and planar structures

We can use the rolling up method of the hexagonal nanotube in the case of non-hexagonal nanotubes as well for constructing the connectivity network of the structure and for its adjacency matrix **A**. The connectivity network is determined by the number of unit cell atoms and by their neighbors. From topological point of view it is supposed that a neighbor of a given atom is in the same unit cell as the given atom, or in one of the 8 neighboring cells [66]. Although an affine transformation does not change the neighboring structure of the connectivity network, it can produce, however, orthogonalized and normalized unit cell vectors. Thus we suppose further that the unit cell is described by two orthonormal vectors $\mathbf{a_1}$ and $\mathbf{a_2}$. Let k, 1 and r be three integers then the vector $\mathbf{ka_1} + \mathbf{1a_2}$ points to the unit cell (k, 1), and (k, 1, r) means the *r*-th atom in this unit cell in the same way as before in the case of polyhex structures. The neighbors of the atom (k, 1, r) can be in the unit cells (k, 1), (k +1, 1), (k -1, 1), (k,1 + 1), (k, 1-1), (k +,1 + 1), (k-1,1-1), (k, +1, 1-1) and (k-1, 1+1) where the corresponding types of neighbors in order are of type t =0, 1, 2, 3, 4, 5, 6, 7 and 8. The parameter t is the index of the unit cell and its 8 neighbors. Figure 4 shows non-hexagonal unit cells containing 8, 24, 32 and 60 atoms.

Let us define the super cell with a parallelogram of side vectors $\mathbf{b_1} = m\mathbf{a_1} + n\mathbf{a_2}$ and $\mathbf{b_2} = p\mathbf{a_1} + q\mathbf{a_2}$ where m, n, p and q are integers. The unit vector $\mathbf{a_3} = \mathbf{a_1} \times \mathbf{a_2}$ be the vectorial product of the vectors $\mathbf{a_1}$ and $\mathbf{a_2}$, and thus we obtain the relation $\mathbf{b_1} \times \mathbf{b_2} = (mq-np)\,\mathbf{a_3}$. For the scalar product of vectors $\mathbf{a_1}$ and $\mathbf{a_2}$ we have $\mathbf{a_i} \cdot \mathbf{a_j} = \delta_{ij}$. From the above definitions follows that for the definition of the unit vectors $\mathbf{a_1}$ and $\mathbf{a_2}$ we did not need coordinates.

We say that an atom of coordinates (k, l, r) is in the super cell of vectors $\mathbf{b_1} = m\mathbf{a_1} + n\mathbf{a_2}$ and $\mathbf{b_2} = p\mathbf{a_1} + q\mathbf{a_2}$ if with $\mathbf{c} = k\mathbf{a_1} + l\mathbf{a_2}$ the following relations are valid [66]:
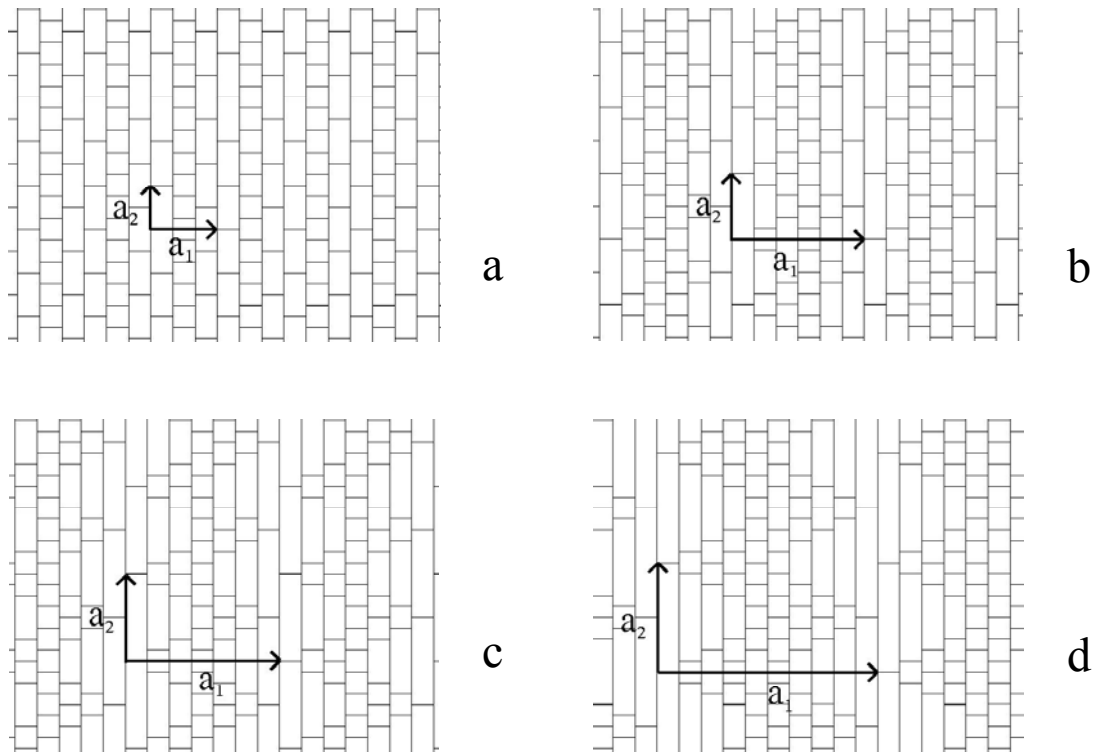
$$\left(\mathbf{b_1} \times \mathbf{b_2}\right) \cdot \mathbf{a_3} = mq - np > 0 \tag{12}$$

$$\left(\mathbf{b_1} \times \mathbf{c}\right) \cdot \mathbf{a_3} = ml - nk \geq 0 \tag{13}$$

$$\left(\mathbf{c} \times \mathbf{b_2}\right) \cdot \mathbf{a_3} = kq - lp \geq 0 \tag{14}$$

$$\left\{\left(\mathbf{c} - \mathbf{b_2}\right) \times \mathbf{b_1}\right\} \cdot \mathbf{a_3} = (k - p)n - (l - q)m > 0 \tag{15}$$

$$\left\{\mathbf{b_2} \times \left(\mathbf{c} - \mathbf{b_1}\right)\right\} \cdot \mathbf{a_3} = p(l - n) - q(k - m) > 0 \tag{16}$$

Figure 4. Neighboring structure of non-hexagonal unit cells containing (a) 8, (b) 24, (c) 32 and (d) 60 atoms.

or

$$\left(\mathbf{b_1} \times \mathbf{b_2}\right) \cdot \mathbf{a_3} = mq - np < 0 \tag{17}$$

$$\left(\mathbf{b_1} \times \mathbf{c}\right) \cdot \mathbf{a_3} = ml - nk \leq 0 \tag{18}$$

$$\left(\mathbf{c} \times \mathbf{b_2}\right) \cdot \mathbf{a_3} = kq - lp \leq 0 \tag{19}$$

$$\left\{\left(\mathbf{c} - \mathbf{b_2}\right) \times \mathbf{b_1}\right\} \cdot \mathbf{a_3} = (k-p)n - (l-q)m < 0 \tag{20}$$

$$\left\{\mathbf{b_2} \times \left(\mathbf{c} - \mathbf{b_1}\right)\right\} \cdot \mathbf{a_3} = p(l-n) - q(k-m) < 0 \tag{21}$$

If the network of a nanotube is constructed by identifying the two $\mathbf{b_2}$ sides (they are parallel with the vector $\mathbf{b_2}$) then the atoms (k_1, l_1, r_1) and (k_2, l_2, r_2) are identified if $r_1 = r_2$ and for the vectors $\mathbf{c_1} = k_1\mathbf{a_1} + l_1\mathbf{a_2}$ and $\mathbf{c_2} = k_2\mathbf{a_1} + l_2\mathbf{a_2}$ the following relation is valid:

$$\mathbf{c_2} - \mathbf{c_1} = u\,\mathbf{b_1} \tag{22}$$

where u is an integer in the range $-1 \leq u \leq 1$.

In the case of toroidal structure each opposite sides of type $\mathbf{b_1}$ and $\mathbf{b_2}$ are identified and the condition for identifying the two atoms(k_1, l_1, r_1) and (k_2, l_2, r_2) is $r_1 = r_2$ and

$$\mathbf{c_2} - \mathbf{c_1} = u\,\mathbf{b_1} + v\,\mathbf{b_2} \tag{23}$$

with integers u and v in the ranges $-1 \leq u \leq 1$ and $-1 \leq v \leq 1$.

The 2-dimensional planar structure is given by the graph of the super cell without rolling up.

From the Equations (12-23) follows that we do not need the special Descartes coordinates of unit cell atoms in a plane for the determination of the connectivity graph $G = (V,E)$. The initial data contain only the integers m, n, p, q and the list of neighbors for each unit cell atoms. A neighboring atom is described by two numbers the serial number r and the type number t. After constructing the graph $G = (V,E)$ for the structure in study we can construct its adjacency matrix **A**.

6. Topological coordinates
6.1 Topological coordinates for fullerenes

With the help of the adjacency matrix **A** we can describe the topological structure of the fullerene given by a graph G = (V, E) but for further investigation usually we need the Cartesian coordinates of the atoms as well. A

simple solution to this problem is the topological coordinate method proposed by Fowler and Manolopoulos [2, 67]. The idea of the topological coordinate method was inspired by Stone's work [68] on bonding in transition-metal clusters. Here we give only the recipe for topological coordinates. The explanations can be found in references [2,23,67, 69-70]. The topological coordinate method is based on the so called bi-lobal eigenvectors of the adjacency matrix **A** of the graph G = (V, E). Eigenvectors having this bi-lobal property can be identified by the graph-disconnection test [69]: for a candidate eigenvector, color all vertices of G = (V, E) bearing positive coefficients black, all bearing negative coefficients white, and all bearing a zero coefficient grey; now delete all grey vertices, all edges connecting a black to a white vertex; if the graph now consists of exactly two connected components, one of black and one of white vertices, then the eigenvector is of bi-lobal.

We arrange in descending order the n = V eigenvalues a_k of the adjacency matrix **A** as:

$$a_1 > a_2 \geq a_3 \geq ... \geq a_n \tag{24}$$

where $\mathbf{c}^k$ is the eigenvector with eigenvalue a_k. The first three bi-lobal eigenvectors $\mathbf{c}^{k1}$, $\mathbf{c}^{k2}$ and $\mathbf{c}^{k3}$ determine the (x_i, y_i, z_i) topological coordinates of the i-th atom by the relations:

$$x_i = S_1 c_i^{k_1} \tag{25}$$

$$y_i = S_2 c_i^{k_2} \tag{26}$$

$$z_i = S_3 c_i^{k_3} \tag{27}$$

with the scaling factors $S_\alpha = 1$ or $S_\alpha = \dfrac{1}{\sqrt{a_1 - a_{k_\alpha}}}$. The most realistic picture

of the fullerene can be found by the scaling factor $S_\alpha = \dfrac{1}{\sqrt{a_1 - a_{k_\alpha}}}$ [71]. In

Figure 3.b is shown the picture of the fullerene C_{100}.   Its coordinates are

topological coordinates obtained by the scaling factor $S_\alpha = \dfrac{1}{\sqrt{a_1 - a_{k_\alpha}}}$ from the

spiral (1,7,12,19,25,28,30,33,36,41,48,50).

6.2 Topological coordinates for torus

Let us suppose that the adjacency matrix **A** describes the topological structure of a torus given by the graph G = (V, E). The position of a point on the surface of a torus is given as the sum of two vectors **R** and **r**. The vector **R** points from the centre of gravity of the torus to a point on the circular spine,

and the vector $\mathbf{r}$ from there to the surface. One can suppose that the vector $\mathbf{R}$ is in the xy plane and $\mathbf{r}$ is in the planes perpendicular to the plane of $\mathbf{R}$. Thus these two vectors are two dimensional planar vectors, each of them can be described by two bi-lobal eigenvectors. If $\mathbf{c}^{k1}$, $\mathbf{c}^{k2}$, $\mathbf{c}^{k3}$ and $\mathbf{c}^{k4}$ are for bi-lobal eigenvectors of $\mathbf{A}$ then the (x_i, y_i, z_i) topological coordinates of the i-th on the torus is given by the relations [23,69]:

$$x_i = S_1 c_i^{k_1}(1 + S_4 c_i^{k_4})$$ (28)

$$y_i = S_2 c_i^{k_2}(1 + S_4 c_i^{k_4})$$ (29)

$$z_i = S_3 c_i^{k_3}.$$ (30)

Namely $R_{i1} = c_i^{k_1}$, $R_{i2} = c_i^{k_2}$, $r_{i1} = c_i^{k_3}$ and $r_{i2} = c_i^{k_4}$. The scaling factors are the same as in the case of fullerenes or the $R_{i1} = c_i^{k_1}$, $R_{i2} = c_i^{k_2}$, $r_{i1} = c_i^{k_3}$ and $r_{i2} = c_i^{k_4}$ parameters are scaled in order to obtain the relations $R = |\mathbf{R_i}|$ and $r = |\mathbf{r_i}|$ where R and r are some average values [23]. Using the non hexagonal unit cell of Figure 4.d. we have calculated the topological coordinates of the tori with the parameters (m, n, p, q) = (1,0,0,5) (Figure 5.a) and with the parameters (m, n, p, q) = (1,-1,5,5) (Figure 5.b).

a   b
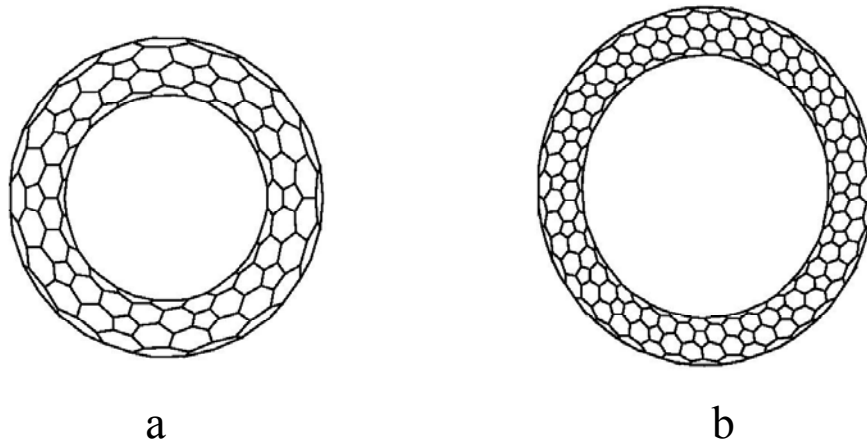
Figure 5. Topological coordinates for tori with parameters (m, n, p, q) = (1,0,0,5) (a) and (m, n, p, q) = (1,-1,5,5) (b). The unit cell is in Figure 4.d.

6.3 Topological coordinates for nanotubes

After cutting the torus by a plane it can be transformed into a tube by the following transformations [23,66,71]:

$$x_i = S_3 c_i^{k_3},$$ (31)

$$y_i = S_4 c_i^{k_4}, \tag{32}$$

$$z_i = R \arccos\left(S_1 c_i^{k_1} / R\right) \quad \text{if} \quad c_i^{k_2} \geq 0 \tag{33}$$

$$z_i = R\left(2\pi - \arccos\left(S_1 c_i^{k_1} / R\right)\right) \quad \text{if} \quad c_i^{k_2} < 0 \tag{34}$$

Here the radius R governs the size of the torus. The vectors $\mathbf{c}^{k1}$, $\mathbf{c}^{k2}$, $\mathbf{c}^{k3}$ and $\mathbf{c}^{k4}$ are the four bi-lobal eigenvectors of the adjacency matrix $G = (V, E)$ characterizing the torus with the parameters (m, n, p, q). From this construction follows, that the obtained tube has the same (m, n, p, q) parameters. The relations (31-34) transform the tori of Figure 5. to the tubes with the parameters (m, n, p, q) = (1,0,0,5) (Figure 6.a) and (m, n, p, q) = (1,-1,5,5) (Figure 6.b).

Supposing forces between the carbon atoms, the nanotubes obtained by the topological coordinate methods of Eqs . (31-34) are not equilibrium structures. We obtained the final relaxed structures with the help of a molecular mechanics method based on the Brenner potential [72]. In this molecular mechanics calculation we supposed interactions only between first neighbor


a   b
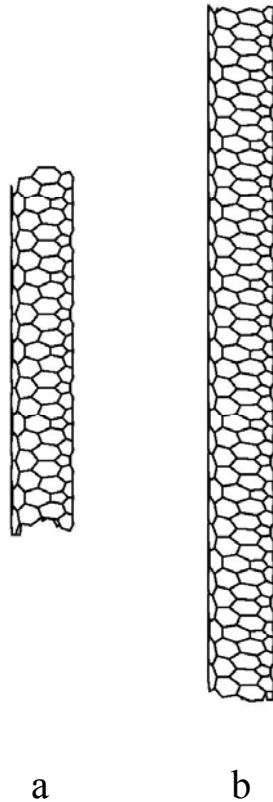
Figure 6. Topological coordinates for nanotubes with parameters (m, n, p, q) = (1,0,0,5) (a) and (m, n, p, q) = (1,-1,5,5) (b). The unit cell is in Figure 4.d.

atoms defined by the $G = (V, E)$ graph of the tube. Here we remark once more that the bi- lobal eigenvectors were obtained from the graph of the auxiliary torus. Figure 7 shows that after relaxation the tube of parameters (m, n, p, q) = (1,0,0,5) turned to be a torus (Figure 7.a) and that of parameters (m, n, p, q) = (1,-1,5,5) turned to be a helical structure (Figure 7.b). In both cases the unit cell was the same (Figure 4.d). This transformation can be explained by the fact that the pentagons correspond to the positive Gaussian curvatures and the heptagons to the negative ones. Thus using a unit cell containing various polygons the shape of the final relaxed structure depends on the unit cell and on the (m, n, p, q) parameters (Figures 7-8).

a   b
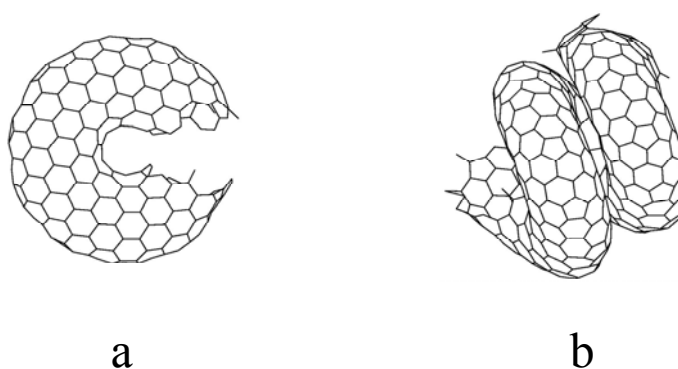
Figure 7. Relaxed structures with parameters (m, n, p, q) = (1,0,0,5) (a) and (m, n, p, q) = (1,-1,5,5) (b). The unit cell is in Figure 4.d.

a   b   c
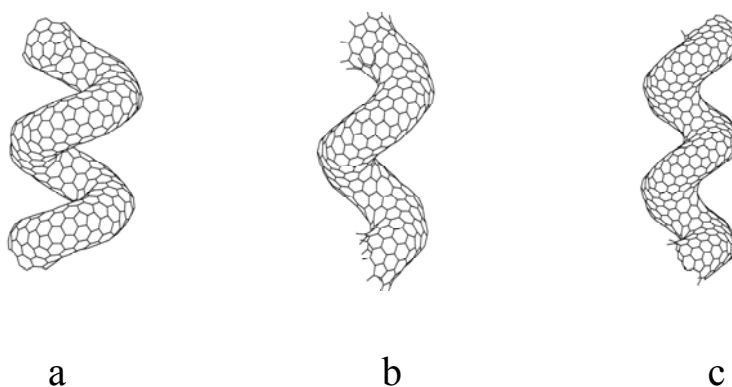
Figure 8. Relaxed structures with parameters (m, n, p, q) = (5,5,-1,1) (a), (m, n, p, q) = (4,2,-2,1) (b), and (m, n, p, q) = (3,1,-3,1) (c). The unit cell is the same for these structures but different of Figure 4.d.

6.4 Topological coordinates for planar structures

On the same way as the torus was transformed to a tube we can transform the tube to a planar structure and we obtain the topological coordinates for the planar structure as [23,66,71]:

$$x_i = r \arccos\left(S_4 c_i^{k_4} / r\right) \quad \text{if} \quad c_i^{k_3} \geq 0, \tag{35}$$

$$x_i = -r \arccos\left(S_4 c_i^{k_4} / r\right) \text{ if} \quad c_i^{k_3} < 0, \tag{36}$$

$$y_i = 0, \tag{37}$$

$$z_i = R \arccos\left(S_1 c_i^{k_{14}} / R\right) \quad \text{if} \quad c_i^{k_2} \geq 0, \tag{38}$$

and

$$z_i = R\left(2\pi - \arccos\left(S_1 c_i^{k_1} / R\right)\right) \quad \text{if} \quad c_i^{k_2} < 0 \tag{39}$$

The radii R and r determine the size and aspect ration of the auxiliary torus, and c^{k1}, c^{k2}, c^{k3}, c^{k4} are four bi-lobal eigenvectors of its adjacency matrix.

In Figure 9. we can see the topological coordinate structures of Figure 4. In Figure 4. only the connectivity network is given. Using Equations (35-39) we obtained Descartes coordinates for drawing unit cells containing non hexagonal polygons. Further results concerning topological coordinates, toroidal and Haeckelite structures can be found in references [58,73-78].
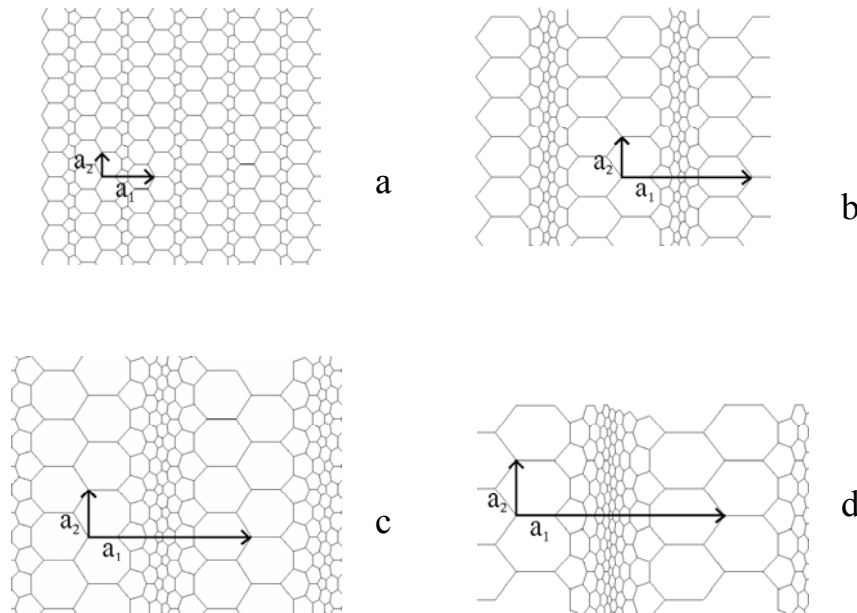
Figure 9. Planar topological coordinates of the unit cells of Figure 4.a (a), Figure 4.b (b), Figure 4.c (c) and Figure 4.d (d).

7. Construction of nanotube junctions
7.1 Nanotube junctions as geometric intersection of cylinders

Although there are various theoretical propositions for nanotube junctions [63-65,79-88], all of them are applied for non chiral structures. Here we

present an algorithm for constructing junctions between single wall nanotubes of any chirality and diameter [40,41]. This method is based on the Geometric Intersection of Cylinders (GIC) and it can describe most of the Y junctions obtained by the Ti-Doped Vapour Catalyst (TDVC) method [62]. Namely in this method new nanotube branches are attached to already developed nanotubes and also the CIG method can be interpreted as attachment of one tube to the other one.

Let us suppose that we want to find the junction between the nanotubes (m_1, n_1) and (m_2, n_2). As the nanotube can be thought of as a cylinder having the hexagonal network on its surface, the junction will be found with the help of intersection of two cylinders. In our notation the line of intersection on the first cylinder is intersection 1 and on the second cylinder is intersection 2. The (u, v) Descartes coordinates with axes $\mathbf{b_1}$ and $\mathbf{b_2}$ for intersection 1 on the rectangle of the first cylinder are:

$$u = r_1 \varphi_1 \tag{40}$$

$$v = \frac{-r_2 \cos(\pi - \varphi_2) + r_1 \cos(\varphi_1)\cos(\alpha)}{\sin(\alpha)} - \frac{r_1}{\tan(\alpha)} \tag{41}$$

and

$$v = \frac{-r_2 \cos(\varphi_2) + r_1 \cos(\varphi_1)\cos(\alpha)}{\sin(\alpha)} - \frac{r_1}{\tan(\alpha)} \tag{42}$$

with

$$\varphi_2 = \arcsin\left(\frac{r_1 \sin(\varphi_1) - d}{r_2}\right) \tag{43}$$

where (r_1, φ_1) and (r_1, φ_2) are the cylindrical coordinates of cylinders 1 and 2. The angle and distance between the axis of the two cylinders are in order α and d. We allow not intersecting axes too. It is supposed further that $r_2 \leq r_1$, $d \leq |(r_1-r_2)|$ and $\arcsin\left(\dfrac{d - r_2}{r_1}\right) \leq \varphi_1 \leq \arcsin\left(\dfrac{d + r_2}{r_1}\right)$.

The same notation is used for the (u, v) coordinates of intersection 2 on the second cylinder rectangle. That is

$$u = r_2 \varphi_2 \tag{44}$$

$$v = \frac{r_1 \cos(\varphi_1) - r_2 \cos(\varphi_2)\cos(\alpha)}{\sin(\alpha)} - \frac{r_1}{\sin(\alpha)} \tag{45}$$
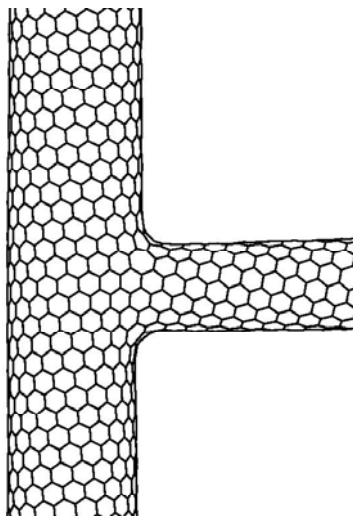
with

$$\varphi_1 = \arcsin\left(\frac{r_2 \sin(\varphi_2) + d}{r_1} \right) \tag{46}$$

where $-\pi \le \varphi \le +\pi$.

These intersection lines cut several carbon-carbon bonds. The vertical and horizontal translations of the intersection lines correspond to axial rotations or translations of the cylinders. By appropriate translations of the cut lines we can reach the case where the number of cut bonds will be the same on the two cylinders. At this case the two cylinders can be joined together along the cut lines and the corresponding half bonds can be joined together as well and the junction can be constructed. The junction of Figure 10 was constructed between the nanotubes (18,2) and (10,5) with the parameters $\alpha = 90^{\circ}$ and d = 0.0Å. See further cases and explanations in references [40,41].

7.2 Nanotube junctions using local coordinates

In the previous paragraph we constructed nanotube junctions between two nanotubes. At a junction, however, can join three or more nanotube as well. In the present paragraph we shall explain the basic ideas of an algorithm that can be used for constructing nanotube junctions between two or more nanotubes of any chirality and diameter, This algorithm will be based on the terminology of manifolds and detailes can be found in references [43,89]. The manifold is a space that, like the surface of the Earth, can be covered by a family of local

Figure 10. Nanotube junction constructed by intersection of cylinders between the nanotubes (18,2) and (10,5) with the parameters $\alpha = 90^{\circ}$ and d = 0.0Å. The junction contains 6 heptagons as non-hexagonal polygons.

coordinate systems. In our case the local coordinate system will be the coordinate system of the hexagonal lattice as defined in Figure 2. If we have for example three tubes at a junctions, we have also three coordinate systems as well, that is we have three local coordinate systems. By constructing the junction one have to tell in which way can we go from one coordinate system to the other. As we suppose that the non hexagonal polygons are at the boundaries of the coordinate systems each of them have two coordinates originated from the neighboring tubes. The common non hexagonal and hexagonal polygons can be visualized as three ribbons, where the polygons are given by the relative local coordinates $\begin{pmatrix} m_1^k \\ n_1^k \end{pmatrix}$ and the corresponding rotations T_i^{+k} on the tube in question and T_i^{-k} on the neighboring tube . Thus ribbon k is the following:

$$\begin{pmatrix} m_1^k \\ n_1^k \end{pmatrix} \frac{T_1^{+k}}{T_1^{-k}} \begin{pmatrix} m_2^k \\ n_2^k \end{pmatrix} \frac{T_2^{+k}}{T_2^{-k}} \begin{pmatrix} m_3^k \\ n_3^k \end{pmatrix} \frac{T_3^{+k}}{T_3^{-k}} \cdots \begin{pmatrix} m_{Nk}^k \\ n_{Nk}^k \end{pmatrix} \frac{T_{Nk}^k}{T_{Nk}^k} \, . \tag{47}$$

For the junction of three nanotubes $\begin{pmatrix} m^1 \\ n^1 \end{pmatrix}$, $\begin{pmatrix} m^2 \\ n^2 \end{pmatrix}$ and $\begin{pmatrix} m^3 \\ n^3 \end{pmatrix}$ exist the following diophantic equations between the parameters of the ribbons k =1, 2 and 3 [43,89]:

$$\sum_{i=1}^{N1}\left(m_i^1 s\left(\sigma_{i-1}^1\right) + n_i^1 s\left(\sigma_{i-1}^1 + 1\right)\right) + s\left(\sigma_{N1}^1\right) -$$

$$\sum_{i=1}^{N2}\left(m_i^2 s\left(\tau_{i-1}^2 + \alpha_{12}\right) + n_i^2 s\left(\tau_{i-1}^2 + \alpha_{12} + 1\right)\right) - s\left(\tau_{N2}^2 + \alpha_{12}\right) = m^1 s\left(\varphi_1\right) + n^1 s\left(\varphi_1 + 1\right) \tag{48}$$

$$\sum_{i=1}^{N1}\left(m_i^1 s\left(\sigma_{i-1}^1 - 2\right) + n_i^1 s\left(\sigma_{i-1}^1 - 1\right)\right) + s\left(\sigma_{N1}^1 - 2\right) -$$

$$\sum_{i=1}^{N2}\left(m_i^2 s\left(\tau_{i-1}^2 + \alpha_{12} - 2\right) + n_i^2 s\left(\tau_{i-1}^2 + \alpha_{12} - 1\right)\right) - s\left(\tau_{N2}^2 + \alpha_{12} - 2\right) = m^1 s\left(\varphi_1 - 2\right) + n^1 s\left(\varphi_1 - 1\right) \tag{49}$$

$$\sum_{i=1}^{N2}\left(m_i^2 s\left(\sigma_{i-1}^2\right) + n_i^2 s\left(\sigma_{i-1}^2 + 1\right)\right) + s\left(\sigma_{N2}^2\right) -$$

$$\sum_{i=1}^{N3}\left(m_i^3 s\left(\tau_{i-1}^3 + \alpha_{23}\right) + n_i^3 s\left(\tau_{i-1}^3 + \alpha_{23} + 1\right)\right) - s\left(\tau_{N3}^3 + \alpha_{23}\right) = m^2 s\left(\varphi_2\right) + n^2 s\left(\varphi_2 + 1\right) \tag{50}$$

$$\sum_{i=1}^{N2}\left(m_i^2 s\left(\sigma_{i-1}^2 - 2\right) + n_i^2 s\left(\sigma_{i-1}^2 - 1\right)\right) + s\left(\sigma_{N2}^2 - 2\right) -$$

$$\sum_{i=1}^{N3}\left(m_i^3 s\left(\tau_{i-1}^3 + \alpha_{23} - 2\right) + n_i^3 s\left(\tau_{i-1}^3 + \alpha_{23} - 1\right)\right) - s\left(\tau_{N3}^3 + \alpha_{23} - 2\right) = m^2 s\left(\varphi_2 - 2\right) + n^2 s\left(\varphi_2 - 1\right) \tag{51}$$

$$\sum_{i=1}^{N3}\left(m_i^3 s\left(\sigma_{i-1}^3\right)+n_i^3 s\left(\sigma_{i-1}^3+1\right)\right)+s\left(\sigma_{N3}^3\right)-$$

$$\sum_{i=1}^{N1}\left(m_i^1 s\left(\tau_{i-1}^1+\alpha_{31}\right)+n_i^1 s\left(\tau_{i-1}^1+\alpha_{31}+1\right)\right)-s\left(\tau_{N1}^1+\alpha_{31}\right)=m^3 s\left(\varphi_3\right)+n^3 s\left(\varphi_3+1\right) \qquad (52)$$

$$\sum_{i=1}^{N3}\left(m_i^3 s\left(\sigma_{i-1}^3-2\right)+n_i^3 s\left(\sigma_{i-1}^3-1\right)\right)+s\left(\sigma_{N3}^3-2\right)-$$

$$\sum_{i=1}^{N1}\left(m_i^1 s\left(\tau_{i-1}^1+\alpha_{31}-2\right)+n_i^1 s\left(\tau_{i-1}^1+\alpha_{31}-1\right)\right)-s\left(\tau_{N1}^1+\alpha_{31}-2\right)=m^3 s\left(\varphi_3-2\right)+n^3 s\left(\varphi_3-1\right) \quad (53)$$

$$\sigma_{N1}^1+\beta_{12}-\tau_{N2}^2-\alpha_{12}=0 \quad \mathrm{mod}(6),\ \sigma_{N2}^2+\beta_{23}-\tau_{N3}^3-\alpha_{23}=0 \quad \mathrm{mod}(6),$$

$$\sigma_{N3}^3+\beta_{31}-\tau_{N1}^1-\alpha_{31}=0 \quad \mathrm{mod}(6) \qquad\qquad (54)$$

Here we have $\sigma_0^k=\tau_0^k=0$, $\sigma_{i+1}^k=\sigma_i^k+T_i^{+k}$ and $\tau_{i+1}^k=\tau_i^k+T_i^{-k}$. The expression $s(\tau)=\dfrac{2}{\sqrt{3}}\sin\left(\dfrac{\pi}{3}\tau+\dfrac{2\pi}{3}\right)$ is a function of the integer variable of τ. The φ_i are generated rotation angles. The number of polygons on ribbon k is Nk and $\alpha_{ij}>0$, $\beta_{ij}<0$ are the direction angles of the ribbons. More details can be found about the solutions of the above mentioned Equations (48-54) in references [43,89].

In Figure 11 three nanotube junction can be seen between various chiral nanotubes. All of them was constructed by the local coordinate method. Figures11.b and 11.c show that the equilibrium structure of the junctions depend on the positions of the non hexagonal nanotubes. In these junctions the tubes are the same but the positions of the six heptagons are different.

a   b   c
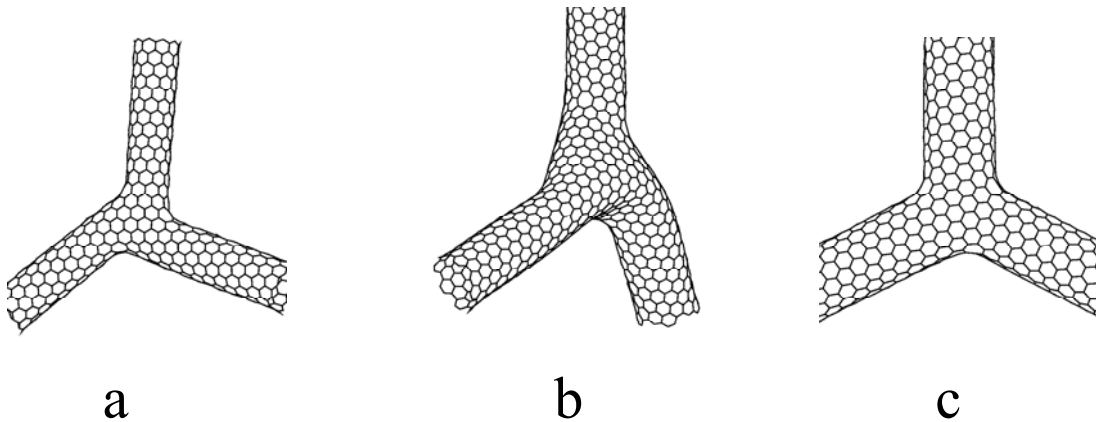
Figure 11. Various nanotube junction constructed by local coordinates of Equations (48-54). The junctions contain 6 heptagons as non-hexagonal polygons. Junctions between nanotubes (10,0), (10,1) and (10,2) (a); (9,6), (8,7) and (10,5) (b); (9,6), (8,7) and (10,5) (c).

8. Conclusions

In the present chapter we have shown several algorithms for generating the connectivity structures of fullerenes nanotubes, nanotube junctions and other hexagonal and non hexagonal carbon surfaces. It was shown that from the topological structures reliable Descartes coordinates can be constructed with the help of the topological coordinate method. Using this topological coordinates preliminary results can be obtained also for the electronic structure [90]. We presented also two algorithms for constructing junctions between nanotubes of any chirality and diameter.

References

1. Kroto, H.W., Heath, J.R., O'Brien, S:C:, Curl, R.F, Smalley, R.E. 1985, Nature, 318, 162.
2. Fowler, P.W., Manolopoulos, D.E. 1995, An Atlas of Fullerenes, Oxford University Press, Oxford.
3. Krätschmer, W., Lamb, L.D., Fostiropoulos, K., Huffman, D.R. 1990, Nature, 347, 354.
4. Iijima S. 1991, Nature, 354, 56.
5. Iijima S., Toshinari I. 1993, Nature, 363, 603.
6. Bethune, D.S., Kiang, C.H., De Vries M.S., Gorman, G.,Savoy, R., Beyers, R. 1993, Nature, 363, 605.
7. Journet, C., Maser, W.K., Bernier P., Loiseau A., Lamy de la Chapelle, M., Lefrant, S., Deniard, P., Lee, R., Fischer, J.E. 1997, Nature, 388, 756.
8. Thess, A., Lee, R., Nikolaev, P., Hai, H., Petit, P., Robert, J., Xu, C., Lee, Y.H., Kim, S.G., Rinzerler, A.G., Colbert, D.T., Scuseria, G.E., Tomanek, D., Fischer, J.E., Smalley, R.E. 1996, Science, 273, 483.
9. Cassell, A.M., Raymakers, J.A., Kong, J., Dai, H.J. 1999, J. Phys. Chem. B 103, 6484.
10. Nikolaev P., Bronikowski, M.J., Bradley, R.K., Rohmund, F., Colbert, D.T., Smith, K.A., Smalley, R. E. 1999, Chem. Phys. Lett. 313, 91.
11. Bronikowski, M.J., Willis, P.A., Colbert, D.T., Smith, K.A., Smalley, R. E. 2001, J. Vac. Sci. Technol. A 19, 1800.
12. Ugarte, D. 1992, Nature, 359, 707.
13. Mackay, A.L., Terrones, H. 1991, Nature, 352, 762.
14. Terrones, H., Mackay, A.L. 1992, Carbon, 30, 1251.
15. Terrones, H., Mackay, A.L. 1997, Prog. Crystal Growth and Charact., 34, 25.
16. Vanderbilt, D., Tersoff, J. 1992, Phys. Rev. Lett., 68, 511.
17. Lenosky, T., Gonze, X., Teter, M., Elser, V. 1992, Nature, 355, 333.
18. Dunlap, B.I., 1992, Phys. Rev. B, 46, 1933.
19. Itoh, S., Ihara, S., Kitakami, J. 1993, Phys. Rev. B, 47, 1703.
20. Itoh, S., Ihara, S., Kitakami, J. 1993, Phys. Rev. B, 47, 12908.
21. Ihara, S., Itoh, S., Kitakami, J. 1993, Phys. Rev. B, 48, 5643.
22. László, I., Rassat. A. 2001, Int. J. Quantum Chem. 84, 136.
23. László, I., Rassat. A. 2003, J. Chem. Inf. Comput. Sci. 43, 519.

24. László, I., Rassat. A. 2003, in Molecular Nanostructures, Kuzmany, H., Fink, J., Mehring, M., Roth, S. (Eds.), AIP Conference Proceedings 685, American Institute of Physics, Melville, New York, page 423.
25. Liu, J., Dai, H.,Hafner, J.H., Colbert, D.T., Tans, S.J., Dekker, C. 1997, Nature 385, 780.
26. Ahlskog, M., Seynaeve, E., Vullers, R.J.M., Van Haesendonck, C., Fonseca, A., Hernadi, K., Nagy, J.B. 1999, Chem. Phys. Lett. 300, 202.
27. Martel, R., Shea, H.R., Avouris, P., 1999, Nature, 398, 299.
28. Sano, M., Kamino, A., Okamura, J., Shinkai, S. 2001, Science, 293, 1299.
29. Cohen, A.E., Mahadevan, L. 2003, PNAS, 100, 12141.
30. Wang, Y., Maspoch, D., Zou, S., Schatz, C., Smalley, R.E. Mirkin, C.A. 2006, PNAS, 103, 2026.
31. Amelinckx, S., Zhang, X.B., Bernaerts, D., Zhang, X.F., Ivanov, V., Nagy, J.B. 1994, Science, 265, 5172.
32. Terrones, H., Terrones, M., Hernández, E., Grobert, N.,Charlier, J-C., Ajayan, P. M. 2000, Phys. Rev. Lett., 84, 1716.
33. Balaban, A.T., Klein, D.J., Liu, X.   1994, Carbon, 32, 357.
34. Terrones ,H., 1994, J. Math. Chem. 15, 143.
35. Ge, M., Satter, K. 1994, Chem. Phys. Lett. 220, 192.
36. Krishnan, A., Dujardin, E., Treacy M.M.J., Hugdahl, J., Lynum, S., Ebbesen, T.W. 1997, Nature 388,451.
37. Iijima, S., Yudasaka, M., Yamada, R., Bandow, S., Suenaga, K., Kokai, F., Takahashi, K.. 1999, Chem. Phys. Lett. 309, 165.
38. Scuseria, G.E. 1992, Chem. Phys. Lett. 195, 534.
39. Chernozatonskii, L. 1992, Phys. Lett. A 172, 173.
40. László, I. 2005, Fullerenes, Nanotubes, And Carbon Nanostructures, 13, 535.
41. László, I. 2005, Croatica Chemica Acta, 78, 217.
42. László, I. 2006, Phys. Stat. Sol (b), 243, 3468.
43. László, I. 2007, Croatica Chemica Acta, xx, xxx.
44. Zhou, D., Seraphin, S. 1995, Chem. Phys. Lett. 238, 286.
45. Nagy, P., Ehlich, R., Biro, L.P., Gyulai, J. 2000, Appl. Phys. A, 70, 481.
46. Bíró, L., Ehlich, R., Osváth, Z., Koós, A., Horváth, Z.E., Gyulai, J., Nagy, J.B. 2002,Mater. Sci. Eng. C 19, 3.
47. Li, J., Papadopoulos, Xu, J.M. 1999, Nature, 402, 253.
48. Satishkumar, B.C., Thomas, P.J.,Govindaraj, A., Rao, C.N.R. 2000, Appl. Phys. Lett. 77, 2530.
49. Deepak, F.L., P.J.,Govindaraj, A., Rao, C.N.R. 2001, ChemPhys. Lett. 354, 5.
50. Klusek, Z., Datta, S., Byszewski, P., Kowalczyk, P., Kozlowski, W. 2002, Surf. Sci., 507-510, 577.
51. Osváth, Z., Koós, A.A., Horváth, Z.E., Gyulai, J., Benito, A.M., Martínez, M.T., Maser, W.K., Bíró, L.P. 2002, Chem. Phys. Lett. 365, 338.
52. Coluci, V.R., Galvão, D.S., Jorio, A. 2006, Nanotechnology, 17, 617.
53. Coluci, V.R.,Dantas, S.O., Jorio, A., Galvão, D.S. 2007, Phys. Rev. B, 75, 075417.
54. Smith, B.W., Monthioux, M., Luzzi, D.E. 1998, Nature, 396, 323.

55. Dresselhaus, M.S., Dresselhaus, G., Eklund, P.C. 1996, Science of Fullerenes and Carbon Nanotubes: Their Properties and Applications, Academic Press, New York, London.
56. Grobert, N. 2007, Materials Today, 10, 28.
57. Bernholc, J., Brenner, D., Nardelli, M.B., Meunier, V., Roland, C. 2002, Annu. Rev. Mater. Res. 32, 347.
58. Lambin, Ph., Bíró, L.P. 2003, New Journal of Physics, 5, 141.
59. Terrones, H., Terrones M. 2003, New Journal of Physics, 5, 126.
60. Chernozatonskii, L. 2003, Journal of Nanoparticle Research, 5, 473.
61. Bíró, L.P., Horváth, Z.E., Márk, G.I., Osváth, Z., Koós, A.A., Benito, A.M., Maser, W., Lambin, Ph. 2004, Diam. and Rel. Materials, 13, 241.
62. Gothard, N., Daraio, C., Gaillard, J., Zhidan, R., Jin, S., Rao, A.M. 2004, Nano Lett. 4, 213.
63. Crespi, V.H. 1998, Phys. Rev. B, 58, 12671.
64. Melchor, S., Khokhriakov, N.V., Savinskii, S.S. 1999, Mol. Eng. 8, 315.
65. Kirby, E.C. 2003, MATCH-Commun. Math. Comp. Chem., 48, 179.
66. László, I. 2005, in Nanostructures: Novel Architecture, Diudea, M.V. (Ed.), Nova Science Publishers, Inc. , New York, page 193.
67. Manolopoulos, D.E., Fowler, P.W. 1992, J. Chem. Phys. 96, 7603.
68. Stone A.J. 181, Inorg. Chem. 20, 563.
69. László, I., Rassat, A., Fowler, P.W., Graovac, A. 2001, Chem. Phys. Lett.. 342, 369.
70. László, I. 2004, Carbon 42, 983.
71. László, I. 2004, in Frontiers of Multifunctional Integrated Nanosystems, Buzaneva, E., Scharff, P. (Eds.), NATO Science Series, II. Mathematics, Physics and Chemistry, 152, 11.
72. Brenner, D.W. 1990, Phys. Rev. B 42, 9458.
73. Graovac, A., Plavšić, D., Kaufman, M., Pisanski, T., Kirby, E.C. 2000, J.Chem.Phys. 113, 1925.
74. Bíró, L.P., Márk, G.I., Koós, A.A., Nagy, J.B., Lambin, Ph. 2002, Phys. Rev. B 66, 165405.
75. Bíró, L.P. Márk, G.I. Koós, A.A., Horváth, Z.E., Szabó, A., Fonesca, A., Nagy, J.B., Colomer, J.F., Lambin, Ph., Meunier, V., Charlier, J.C., Bedoya-Martínez O.N., Hernández, E. 2005, Fullerenes, Nanotubes, and Carbon Nanostructures, 13, 523.
76. Diudea, M.V., 2002, Bul. of the Chem. Soc. of Japan 75, 487.
77. Diudea, M.V., 2002, Phys. Chem. Chem. Phys. 4, 4740.
78. Diudea, M.V., John, P.E, Graovac, A., Primorac, M., Pisanski, T. 2003, Croatica Chemica Acta, 76, 153.
79. Chico, L., Crespi, V.H., Benedict, X.L., Louie, S.G., Cohen, M.L. 1996, Phys. Rev. Lett. 76, 971.
80. Menon, M. 1997, Phys. Rev. Lett. 79, 4453.
81. Treboux, G., Lapstun, P., Silverbrook, K. 1999, Chem. Phys. Lett. 306, 402.
82. Andriotis, A.N., Menon, M., Srivastava, D., Chernozatonskii, L., 2001, Appl. Phys. Lett. 79, 266.
83. Andriotis, A.N., Menon, M., Srivastava, D., Chernozatonskii, L., 2001, Phys. Rev. Lett. 87, 66802.

84. Andriotis, A.N., Menon, M., Srivastava, D., Chernozatonskii, L., 2002, Phys. Rev. B. 65, 165416.
85. Terrones, M., Banhart, F., Grobert, N., Charlier, J.-C., Terrones, H., Ajayan, P.M. 2002, Phys. Rev. Lett. 81, 5234.
86. Meunier, V., Nardelli, M.B., Berholc, J., Zacharia, T., Charlier, J.-C. 2002, Appl. Phys. Lett. 81, 5234.
87. Zsoldos, I., Kakuk, Gy., Réti, F., Szász, A. 2004, Modeling and Simul in Mat. Sci. and Eng. 12, 1251.
88. Zsoldos, I., Kakuk, Gy., Janik, J., Pék, L. 2005, Diam. Relat. Mater 14, 763.
89. László, I. 2007, Phys. Stat. Sol (b), xxx, xxx.
90. László, I. 2004, J. Chem. Inf. Comput. Sci. 44, 315.